JOURNAL OF Applied Polymer SCIENCE

Latex-templated biomineralization of silica nanoparticles with porous shell and their application for drug delivery

Huizhi Zhou, Jingchi Luo, Qing Gao, Tingting Yang
Hubei Collaborative Innovation Center for Advanced Organic Chemical Materials, Faculty of Materials Science and Engineering, Hubei University, Wuhan 430062, China
Correspondence to: T. Yang (E-mail: ytt_ytt@sina.com)

ABSTRACT: A latex-templating method for synthesizing the core-shell silica nanoparticles (NPs) with porous shell was developed via biomineralization in the presence of poly[2-(methacryloyloxy)ethyl] trimethylammonium chloride (pDMC)-modified polystyrene latex. Calcination of the as-obtained SiO_2 NPs led to the removal of the latex core and consequently to hollow silica NPs with porous shell. In particularly, the microstructure and thickness of silica shell could be controlled by simply changing the reaction parameters of silicification. Furthermore, facile encapsulation of a drug molecules and its sustained release were demonstrated. © 2016 Wiley Periodicals, Inc. J. Appl. Polym. Sci. **2016**, *133*, 44200.

KEYWORDS: composites; drug delivery systems; nanostructured polymers; porous materials

Received 6 January 2016; accepted 17 July 2016
DOI: 10.1002/app.44200

INTRODUCTION

Silica nanomaterials have attracted expanding interests mainly due to their outstanding properties, such as excellent mechanical and thermal stability, easy modification, low toxicity and high biocompability,[1] especially for the core-shell silica NPs, giving a rise to potential applications of catalysis,[2] biological imaging,[3] controlled drug delivery,[4] and adsorption diagnostic.[5] Up to now, there are two approaches to obtain the core-shell silica nanostructures. One is the self-assembly of surfactants with different compositions or the supramolecular assembly based on molecular recognition,[6] and another is based on surface reactions or precipitation/deposition on the preformed nano-objects through electrostatic intereaction,[7] covalently grafting,[8,9] or affinity coating.[10] For instance, Mandal and Kruk had performed the silica deposition into the shell domain of the individual micelles assembled by block copolymers.[11] Whitaker and Furst reported the synthesis of silica@polystyrene particles with multilayered shells by consecutively assembling silica NPs and poly(allylamine) hydrochloride onto the colloids based on the layer-by-layer self-assembly technique.[12] Graf had used poly(*N*-vinylpyrrolidone) as a coupling agent to anchor the silica shell onto polystyrene NPs by a sol-gel process.[13] However, the above-mentioned methods of silica formation variously incorporate some nonideal conditions, including the use of acidic or basic pH and elevated temperature, or the large waste of templates and/or organic cosolvents.[14,15] Moreover, the modification and synthetic procedure of silica nanostructure is tedious and time-consuming.

On contrast, silica biomineralization in nature happens under more environment-friendly conditions, such as room temperature, near neutral pH, and the aqueous environment with high efficiency. Amounts of studies have testified that polyamine is the key functional group for catalyzing silica deposition.[16] Yuan et al. described using cationic polyamine-based block copolymer micelles as colloidal templates to direct the synthesis of silica hybrid NPs of around 35 nm diameter.[17] Yang et al. had used the polystyrene latex assisted adsorbed with poly-L-lysine as templates to catalyze silica mineralization.[18] However, how to accurately control the morphology and chemical composition of silica NPs during mineralization period is still a big challenge. As we know, template-directed synthesis is just a copy process. The advanced synthetic strategies in the polymer colloid science open us a convenient door to obtain the particles with the certain size, morphology, and composition whatever we wanted to be used as templates. Compared with the noncovalent-driven self-assemblies as templates, emulsion polymerization techniques can provide an alternative pathway achieving more stable and versatile latex with tunable chemical composition and diverse morphology. The polyamine-based hydrophilic microgel[19] and core-shell latex[20] covalently bonding DMC and 2-diethylamino ethyl methacrylate (DEA) chains, respectively, were served as scaffold for silica deposition. To the best of our knowledge, polystyrene (pSt) latex covalently modified cationic pDMC capable of both stabilizing latex templates and catalyzing biosilicification around the latex core have not been reported,

Table I. Synthetic Conditions and Compositions of pSt-*co*-pDMC@SiO_2 Nanoparticles

Run	DMC (wt %)	*P*:*T*	Time (h)	SiO_2 content (wt %)	Diameter[a] (nm)	Diameter[b] (nm)	Thickness of silica shell[b] (nm)	Zeta potential (mV)
1	2	1:20	12	33.16%	116.1	105.47 ± 8	3.94 ± 0.50	−12.8
2	2	1:50	12	40.49%	132.3	108.48 ± 4	5.44 ± 0.71	−14.1
3	2	1:50	9	33.70%	124.7	106.60 ± 7	4.30 ± 0.53	−13.7
4	2	1:50	5	29.47%	121.3	103.13 ± 6	2.75 ± 0.38	−10.6
5	5	1:50	12	41.91%	124.5	96.37 ± 8	5.96 ± 0.62	−19.8
6	30	1:50	12	43.75%	156.4	89.76 ± 12	6.47 ± 0.76	−17.5
7	50	1:50	12	44.82%	194.1	—	—	−33.3

[a] Obtained by DLS.
[b] Obtained by TEM, analyzed more than 100 particles

especially to the fabrication silica NPs with porous shell without adding any pore-forming agents.

In this article, the uniform cationic pSt latex modified by pDMC chains had been synthesized and used as hard templates for silica biomineralization, which leading to the facile formation of core-shell pSt-*co*-pDMC@SiO_2 hybrid NPs, and nontemplated silica was obtained. The influence of reaction parameters of mineralization on the change of microstructure and thickness of silica shell have been investigated in detail. Calcination treatment of the as-synthesized SiO_2 hybrid NPs led to the removal of the scarified polymer core to obtain the hollow SiO_2 ($HSiO_2$) NPs with porous shell. Aspirin had been adopted as the loading drug into the $HSiO_2$ NPs to investigate theirs *in vitro* drug-release behavior.

EXPERIMENTAL

Materials

Styrene (St; 99%; sinopharm chemical Reagent Co., Ltd) was distilled under vacuum and stored at −5 °C before use. [2-(Methacryloyloxy)ethyl] trimethylammonium chloride solution (DMC; 75 wt % in H_2O) and acetylsalicylic acid (aspirin; 99%) were purchased from Aladdin. 2,2′-Azobis[2-methylpropionamidine] dihydrochloride (AIBA) and tetramethyl orthosilicate (TMOS; ≥95%) were obtained from ACROS. Ethanol absolute was purchased from Tianjin Bodi Chemicals Co., Ltd. Phosphate-buffered saline solution (PBS; NaCl 137 mmol/L, KCl 2.7 mmol/L, Na_2HPO_4 4.3 mmol/L, KH_2PO_4 1.4 mmol/L, pH 7.2, at 25 °C). Deionized water was used in all experiments.

Synthesis of pSt-*co*-pDMC Latex

The pSt-*co*-pDMC latex with different incorporation concentration of DMC were synthesized by surfactant-free emulsion polymerization. Typically, the polymerization was performed in a 0.25 L four-necked kettle equipped with mechanical stirrer, thermometer, reflux condenser and inlet system of nitrogen. 100 mL deionized water, 10 g St, and a certain amount of DMC (see Table I) were charged into the kettle at room temperature followed by purged with nitrogen for 30 min. Then the resulted pre-emulsion system was added 10 mL AIBA aqueous solution (10 mg mL^{-1}) and heated to 75 °C for 5 h. The total conversion of monomers was determined gravimetrically to be about 90 wt %. A 0.25 wt % pSt-*co*-pDMC emulsion was prepared by dispersing the prepared emulsion in water with the aid of ultrasonic bath.

Synthesis of pSt-*co*-pDMC@SiO_2 NPs

The synthesis was adapted from an experimental procedure published earlier.[20] A desired amount of TMOS was dispersed with 20 mL pSt-*co*-pDMC emulsion (0.25 wt %) to start the growth of silica shell. The nanocomposite particles were aged for typical 12 h using magnetic stirring at room temperature, and purified by several cycles of centrifugation with 15,000 rpm for 30 min and cautious redispersion in ethanol. The products were dried overnight under a vacuum.

Synthesis of $HSiO_2$ NPs with Porous Shell

Finally, the pSt-*co*-pDMC@SiO_2 NPs were calcined by heating to 600 °C at a heating rate of 20 °C/min, and keeping at this temperature for 2 h in order to completely remove the latex core and get pure silica NPs with hollow structure.

Preparation of Drug-Loaded $HSiO_2$ NPs

The drug loading and *in vitro* release profiles were obtained from earlier reports.[21] Nonsteroidal anti-inflammatory aspirin was chosen as the model drug. Hundred milligrams of aspirin powder was added into 20 mL PBS and fully agitated for 24 h. Then 10 mg of $HSiO_2$ NPs was added into the mixture to further stir for another 24 h at 37 °C. The aspirin-loaded sample (Aspirin@$HSiO_2$) was separated from the above mixture by centrifugation at 6000 rpm, and then washed three times with PBS. The products were dried overnight under a vacuum. The drug loading efficiency (LE) can be calculated as follows:

$$\text{LE } \% = (M_0 - M_1)/M_0 \times 100\%$$

where M_0, M_1 represented the drug concentration before and after loading.

In Vitro Drug Release Study

The *in vitro* release behavior of Aspirin from $HSiO_2$ NPs at different pH was monitored by dialysis bag diffusion techniques. 10 mg Aspirin@$HSiO_2$ were first mixed with 10 mL PBS and then placed into a dialysis bag (molecular weight cutting = 3500 g/mol). Then the dialysis bag was immersed into 250 mL PBS and stirred at 37 °C in a separated baker. Drug release started when the dialysis bag was put into PBS. 5 mL PBS was

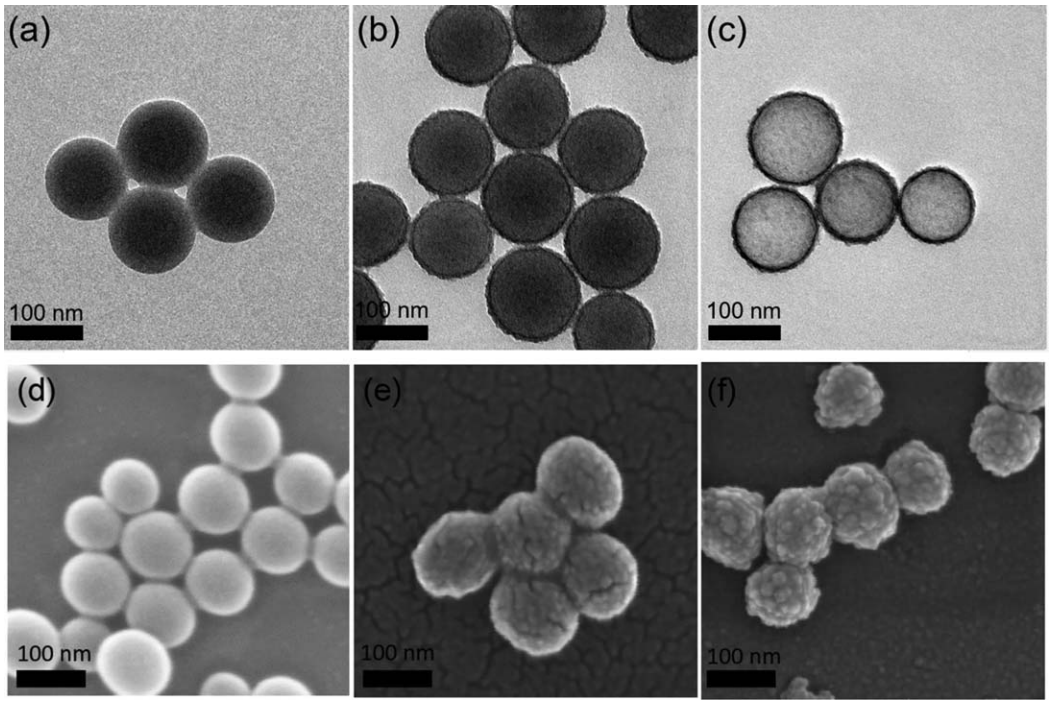

Figure 1. Typical TEM and SEM images of (a) and (d) pSt latex modified with 2 wt % DMC; (b) and (e) pSt-*co*-pDMC@SiO_2 hybrid NPs synthesized by using (A) as templates, $P{:}T = 1{:}20$, 12 h; (c) and (f) $HSiO_2$ NPs synthesized by calcination (b) at 600 °C.

taken out from the drug release system every hour to exam the extent of drug release and add 5 mL fresh PBS in. The amount of the drug release was evaluated by monitoring the absorption of aspirin in the solution by UV/Vis absorption spectroscopy at a wavelength of 296 nm.

Characterization

Malvern Zetasizer instrument (HPPS5001) was used for dynamic light scattering measurements on highly dilute aqueous nanoparticle dispersion. Thermogravimetric measurements were performed in a Perkin-Elmer Diamond TG/DTA instrument at a heating rate of 10 °C/min. TEM studies were operated on Tecnai G20 microscope (FEI Corp.). SEM images were recorded on FE-SEM instrument (JEOL JSM-6700F). Aqueous electrophoresis measurements were operated on Malvern Zetasizer NanoZS instrument. The surface areas of the $HSiO_2$ NPs were estimated from N_2 adsorption-desorption experiments using an Autosorb-1-MP surface area analyzer (Quantachrome Company). UV–Vis spectroscopy (Perkin-Elmer Lambda17) was used to analyze the drug loading efficiency and drug release of Aspirin.

RESULTS AND DISCUSSION

Controlled Synthesis of the Core-Shell pSt-*co*-pDMC@SiO_2 NPs

In nature amino-based peptides or protein plays an important role in accuracy control the rapid deposition of silica.[22] Previous studies has demonstrated that the synthetic amino-functioned polymers, such as poly-L-lysine,[23] polyethyleneimine,[24] and poly(allylamine hydrochloride),[25] have the same ability to guide silicification under more ambient conditions in the presence of suitable templates.

In the typical synthetic process, the uniform pSt latex covalently modified with cationic pDMC chains was chosen as bifunctional templates, followed by mixture with TOMS to initiate silica biomineralization, and resulted to obtain pSt-*co*-pDMC@SiO_2 NPs and $HSiO_2$ after removing the latex components. Figure 1 showed the typical TEM and SEM images of pSt-*co*-pDMC latex (a/d), pSt-*co*-pDMC@SiO_2 NPs (b/e), and $HSiO_2$ NPs (c/f), respectively. Silicification formed a coarse shell in the thickness of ~10 nm around the smooth pSt-*co*-pDMC latex core, which exhibit a distinct core-shell morphology. The number-average diameter of the pSt-*co*-pDMC@SiO_2 NPs was calculated to be 108.48 ± 4 nm by analyzing more than 100 particles, while DLS studies indicated an intensity-average diameter of 132 nm at 25 °C. The size of pSt-*co*-pDMC@SiO_2 NPs measured by DLS were larger than those determined by TEM, due to the surrounding water molecules and swelling of pDMC chains. Furthermore, neither free latex templates nor nontemplated silica was observed, which means the SiO_2 deposition occurred exclusively on the surface of latex templates.

The well-defined spherical $HSiO_2$ NPs were obtained after calcination, and EDX spectrum [Figure 2(a)] of randomly-selected $HSiO_2$ showed the distinguish peaks of Si and O elements. TGA curves [Figure 2(b)] of pSt-*co*-pDMC@SiO_2 NPs (Run 1) showed the mass ratio of silica was about 33.16%.

Zeta potential of pSt-*co*-pDMC latex and pSt-*co*-pDMC@SiO_2 NPs was examined by aqueous electrophoresis measurements. As shown in Figure 2(c), the pSt-*co*-pDMC latex exhibited positive zeta potentials in the pH range from 2 to 12 due to the cationic character of pDMC chains, which mean the surface of the pSt latex was covered a pDMC layer to provide a favorable condition for silica deposition *in situ*. In contrast, pSt-*co*-pDMC@SiO_2 NPs exhibited negative zeta potentials in the same

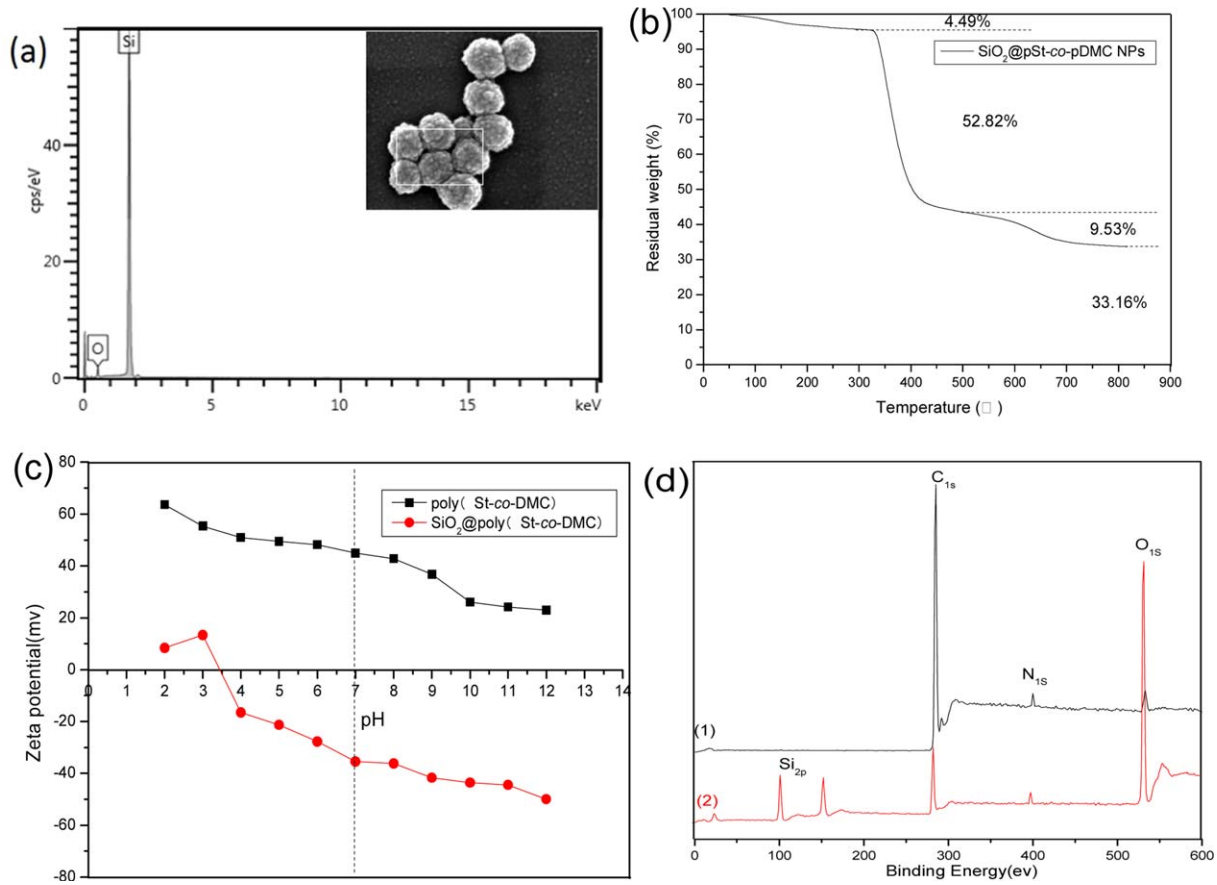

Figure 2. (a) EDX spectrum of $HSiO_2$ NPs, the insert figure is the SEM image of $HSiO_2$. (b) A TGA curve of pSt-*co*-pDMC@SiO_2 hybrid NPs. (c) Zeta potential versus pH curves; (■) pSt-*co*-pDMC latex, (●) pSt-*co*-pDMC@SiO_2. (d) XPS profiles of (1) pSt-*co*-pDMC latex with 2 wt % DMC and (2) pSt-*co*-pDMC@SiO_2 NPs synthesized by (1) as template under *P*:*T* = 1:20, 12 h. [Color figure can be viewed in the online issue, which is available at wileyonlinelibrary.com.]

pH range, reflecting the anion nature of the silanol groups due to the deposition of silica onto the cationic network. This evident change of surface charge inferred that the silica deposition was occurred on the surface of latex templates.

The chemical composition of pSt-*co*-pDMC@SiO_2 NPs were further studied by XPS. As shown in Figure 2(d), the additional peak value at 104.09 eV (Si_{2p}) was only observed in the spectrum of pSt-*co*-pDMC@SiO_2 NPs, but the peak value at 399.9 eV (N_{1s}) from pDMC was observed in the spectra of both pSt-*co*-pDMC and pSt-*co*-pDMC@SiO_2 NPs. This indicated that the silica shell was hybrid with the polyamine chains because the hydrophilic the pDMC segments intent to form hairy shell attached to pSt latex.

The synthesized recipes and composition of the pSt-*co*-pDMC@SiO_2 hybrid NPs were summarized in Table I. The pSt latex had significant cationic and hydrophilic character due to the pDMC modification, so it could act as a bifunctional templates capable of both catalyzing biosilicification under ambient conditions and serving as the physical scaffold for silica deposition. By simply changing the biomineralization conditions, including the mass ratio of DMC to St (*D*/*S* ratio), TMOS amount (namely, the mass ratio of polymer to TMOS, *P*:*T*) and reaction time, the pSt-*co*-pDMC@SiO_2 NPs with tunable nanostructure and chemical composition could be obtained.

The *D*/*S* ratio was varied from 2 wt %, 5 wt %, 30 wt %, and 50 wt % to observe effects on the incidence of pSt-*co*-pDMC latex morphology. As showed in Figure 3(a–d), the TEM images revealed that with increasing the mass amount of the hydrophilic cationic monomer DMC, the surface of pSt latex became blurring and sticky, so it was difficult to see the profile of pSt latex while the *D*/*S* ratio was higher to 50 wt %. *D*/*S* ratio seemed have more impact on the silicification process. As shown in Figure 3(e–g), the pSt-*co*-pDMC@SiO_2 NPs prepared by templates with low *D*/*S* ratio had uniform ball-like core-shell morphology and their surfaces were smooth and regular. However, the surfaces became rougher and irregular with increasing *D*/*S* ratio. When the *D*/*S* ratio was beyond 30 wt %, the pSt-*co*-pDMC@SiO_2 NPs had a strawberry-like surface morphology.

It was noteworthy that the diameter of pSt template was decreased with increasing *D*/*S* ratio, because that the superfluous DMC could serve the surfactant besides of the modification monomer, which induced more entanglement of template latex. So we chose the latex with low *D*/*S* ratio of 2 wt % as templates to proceed the further experiments investigating the effect of TMOS amount and reaction time. Previous reports indicate that the mount of silica precursor is a key parameter to influence of the thickness of silica shell.[19,20] Various TMOS amounts

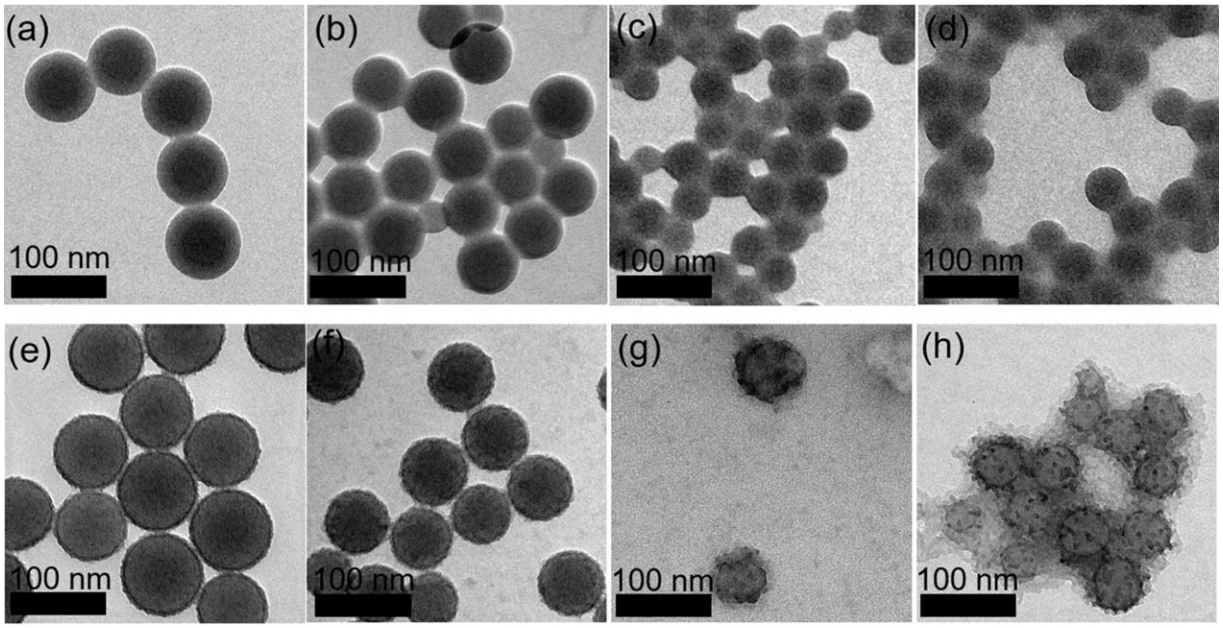

Figure 3. Typical TEM images of pSt-*co*-pDMC latex prepared with various DMC amount, (a) 2 wt %; (b) 5 wt %; (c) 30 wt %; (d) 50 wt %; and TEM image of the pSt-*co*-pDMC@SiO_2 hybrid NPs under the different DMC amount: (e) 2 wt %; (f) 5 wt %; (g) 30 wt %; and (h) 50 wt %, Else otherwise mentioned, polymer: TMOS = 1:50 under 12 h.

(*P*:*T* ratio) were investigated in the synthetic experiments to see the possibility of control the thickness of silica shell. The pSt-*co*-pDMC@SiO_2 NPs were prepared by *P*:*T* = 1:20 and 1:50 under 2 wt % *D*/*S* ratio and 12 h. The thickness of SiO_2 shell estimated from TEM images in Figure 4(c,d) were thin and equal to 5.44 nm and 3.94 nm, respectively. TGA studies

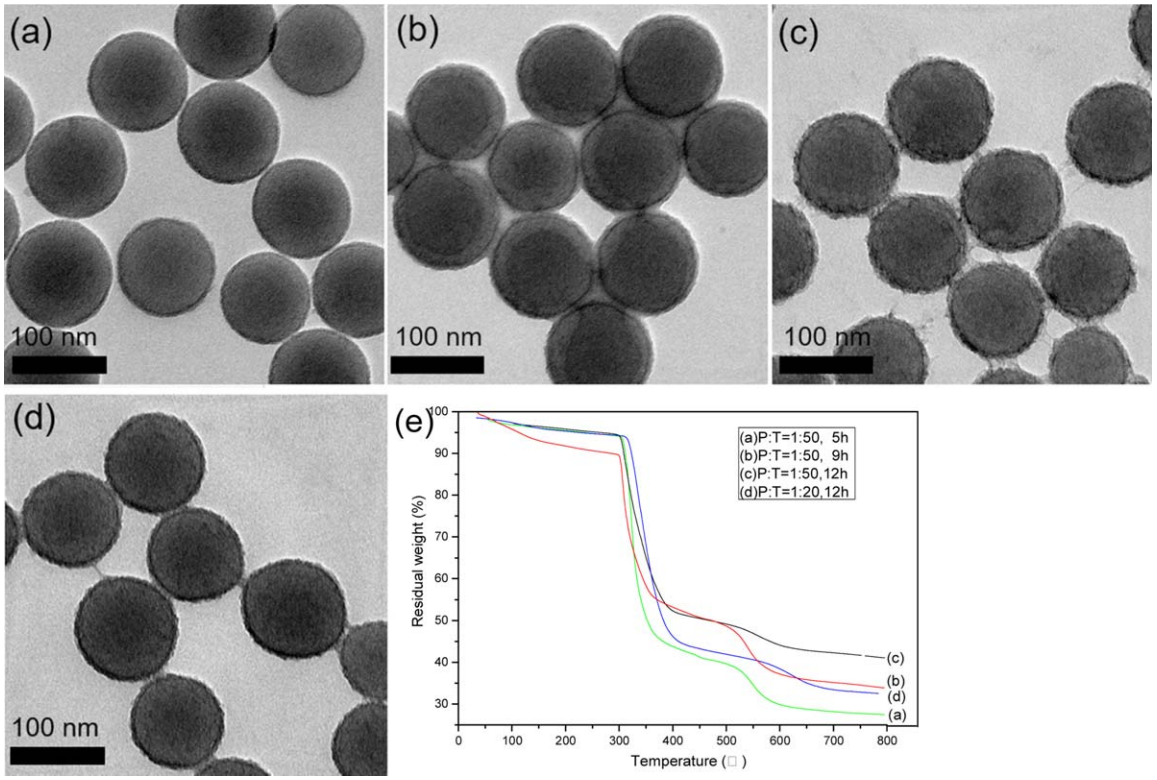

Figure 4. TEM image of pSt-*co*-pDMC@SiO_2 nanoparticles synthesized by (a) 5 h, (b) 9 h, (c) 12 h, fixed 2 wt % DMC and *P*:*T* = 1:50; (d) *P*:*T* = 1:20 fixed 2 wt % DMC and 12 h; (e) TGA curves of pSt-*co*-pDMC@SiO_2 nanoparticles synthesized by different reaction time and P:T ratio. [Color figure can be viewed in the online issue, which is available at wileyonlinelibrary.com.]

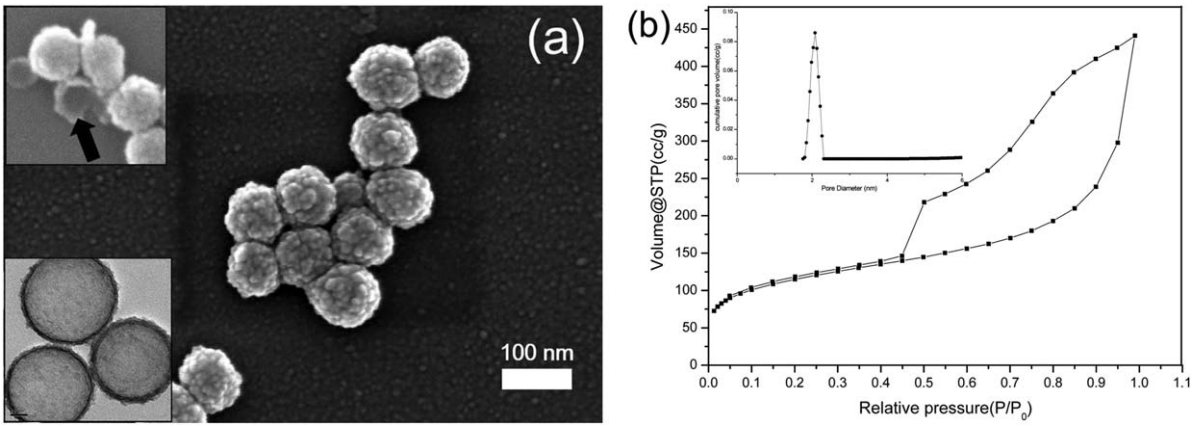

Figure 5. (a) SEM image of $HSiO_2$, insert images are SEM image of fragmental $HSiO_2$ nanoparticles (up) and TEM image of $HSiO_2$ nanoparticles (below); (b) adsorption and desorption isotherms and pore size distribution curve of $HSiO_2$.

showed that the SiO_2 content was about 40.49% for Figure 4(c) and 33.16% for Figure 4(d) in mass, indicating that the increase of TMOS ratio led to higher SiO_2 content in the pSt-*co*-pDMC@SiO_2 NPs, as expected.

Moreover, we found that reaction time also affected strongly the morphology and thickness of silica shell of pSt-*co*-pDMC@SiO_2 NPs. Figure 4(a–c) showed the different TEM images of hybrid silica NPs just prepared under different reaction time of 5 h, 9 h, and 12 h. After 5 h of reactive time, the smooth and thin silica shell apparently formed around the pSt latex templates with a thickness of 8.05 nm. Prolonging reaction time to 9 h and 12 h, the surfaces of pSt-*co*-pDMC@SiO_2 NPs became much rougher, and the thickness of newly synthesized silica shell increased to 9.75 nm and 13.55 nm, respectively. The SiO_2 content of hybrid particles was also increased from around 29.49% to 40.49% in mass, calculated by TGA curves. But the growth of silicon conversion with increasing reaction time ran relatively flat. However, adding more TMOS could not result larger silicon conversion. Therefore, a reasonable TMOS amount and reaction time are crucial for high-efficient formation of pSt-*co*-pDMC@SiO_2 with an excellent morphology.

The Formation Mechanism of $HSiO_2$ with Porous Shell

Here the $HSiO_2$ nanoparticles with cavity could be simply obtained just by calcination at 600 °C. We selected the pSt-*co*-pDMC@SiO_2 nanoparticles (Run 5) to calcine to get well-defined $HSiO_2$. Most $HSiO_2$ nanoparticles maintained the whole spherical structure from the inset TEM image in Figure 5(a), and occurrence of a small amount of fragmentized $HSiO_2$ confirmed the hollow interior. SEM image further revealed that strawberry-like spherical $HSiO_2$ NPs were obtained, which indicated that many silica nanoparticles with tens nanometers size accumulated each other to form the SiO_2 shell, which implied the narrow channel may be exited between the smaller silica nanoparticles.

As shown in Scheme 1, the latex composing pSt-*co*-pDMC have been synthesized by surfactant-free approach, that is, by homogeneous nucleation method. DMC being hydrophilic in nature starts to polymerize first, followed by the polymerization of more hydrophobic styrene. But because the polymer chains from styrene are also hydrophobic in nature, they push the hydrophilic chains of pDMC away to the surface, leading to form the hairy-like shell morphology to guarantee the excellent water-dispersity of pSt latex. Moreover, positively charged pDMC chains may interact electrostatically with silanolate at neutral pH, which in turn act as nucleation sites and direct silica growth through polycondensation of TMOS. So the large amount of silica nanoparticles with smaller size have been formed simultaneously between pDMC chains, and then accumulated at the interface of pSt latex.

Si_{2p} peak at 104.09 eV and N_{1s} peak at 399.9 eV were both observed in the XPS spectrum of pSt-*co*-pDMC@SiO_2 nanoparticles, which in turn confirmed that the silica shell was hybrid with organic pDMC chains. Calcination post-treated on the pSt-*co*-pDMC@SiO_2 NPs did remove the core components, at the mean time remove the pDMC in the silica shell to generate the porous nanostructure without additional pore-forming agents. BET test indicated that the surface area of $HSiO_2$ was around 388.1 m^2/g [see Figure 5(b)]. The average pore diameter

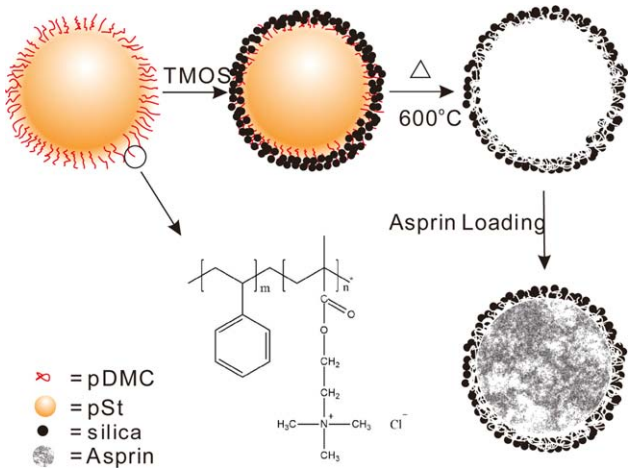

Scheme 1. Schematic representation of the synthesis of silica hybrid nanoparticles with porous shell. [Color figure can be viewed in the online issue, which is available at wileyonlinelibrary.com.]

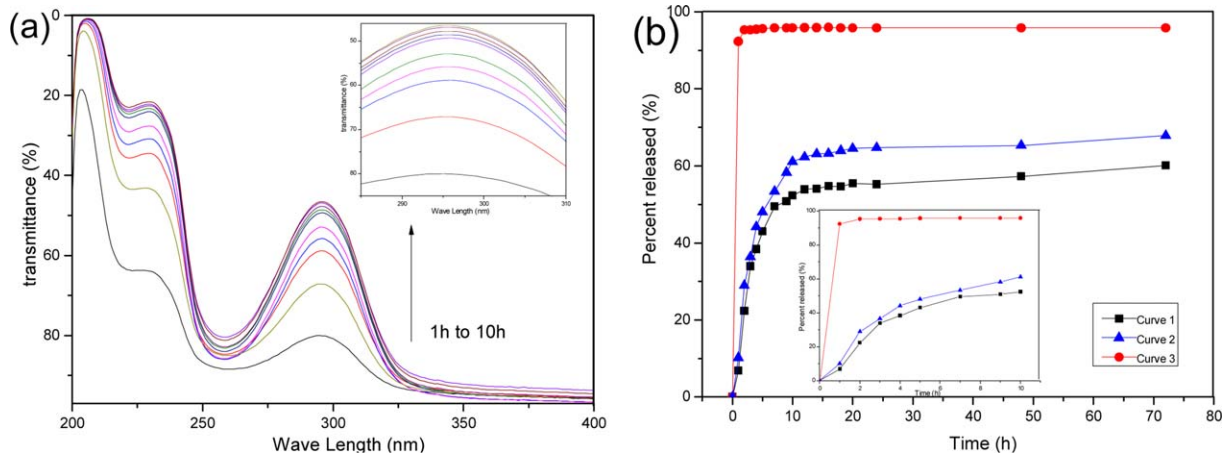

Figure 6. (a) UV-Vis absorption spectra of PBS which used in the process of *in vitro* drug release (Aspirin@$HSiO_2$, pH 7.4, 37 °C) and (b) release profile of the Aspirin@$HSiO_2$ capsules under different pH: pH 7.4 (curve 1) and pH 3.4 (curve 2), as well as of the pure aspirin powder under pH 7.4 (curve 3) over a 80 h period in phosphate-buffered saline at 37 °C. [Color figure can be viewed in the online issue, which is available at wileyonlinelibrary.com.]

was around 3.68 nm and the average pore volume was around 0.168 cm^3/g based on Horvath-Kawazoe (HK) method.

The Drug Release Behavior of Aspirin@$HSiO_2$

The porous structure and hollow interior play a significant role in improving the solubility and decrease release rate of poorly water-soluble drugs.[26,27] We demonstrated facile encapsulation and sustained release profile associated with the $HSiO_2$ nanoparticles using aspirin as a model of poorly water-soluble drug. And the loading capability of each $HSiO_2$ was about 41.06% when the silica shell thickness was about 10 nm.

The sustained release behavior of Aspirin from the $HSiO_2$ was further investigated in phosphate-buffered saline (PBS). Figure 6(a) showed that the height of peak at 296 nm increased slowly after the interaction between PBS with the Aspirin@$HSiO_2$ occurred, which indicating that the loaded aspirin could be released slowly with time increasing. Figure 6(b) showed the release behavior of aspirin from the Aspirin@$HSiO_2$ capsules in PBS at 37 °C under different pH conditions. Compared with pure aspirin powder, the release rates of aspirin from the Aspirin@$HSiO_2$ capsules were remarkably declined, and Aspirin@$HSiO_2$ capsules showed 38.4% (pH 7.4) and 44.2% (pH 3.4) after 4 h. The aspirin release then gradually increased with time. The aspirin loaded $HSiO_2$ nanoparticles showed a faster release rate at pH 3.4 than at pH 7.4, which was important for minimized prenature release. As discussed above, the silica shell thickness could be controlled by changing TMOS amount, if the dependence of drug release rate is on the silica shell thickness, so we can monitor the release rate of $HSiO_2$ under controlled manner. And this need further investigated.

CONCLUSIONS

Well-defined SiO_2 hybrid nanoparticles were facile synthesized using pDMC-modified pSt latex as templates based on biomineralization process. pDMC-modified pSt latex modularized an excellent water-dispersity with biosilicification activity, thus achieving the formation of pSt-*co*-pDMC@SiO_2 nanoparticles under more ambient conditions, including room temperature, neutral pH, and aqueous media. The nanostructure and chemical composition of the resulted pSt-*co*-pDMC@SiO_2 NPs could be controlled by simply adjusting the reaction parameters of mineralization. Calcination to remove the latex templates consequently led to hollow structure with porous shell. Since the available interior cavity and highly permeable porous silica shell were easy for loading the guest species, the $HSiO_2$ had been pursued in drug controllable release. And the results of *in vitro* Aspirin release study demonstrated that the $HSiO_2$ with high loading capacity had a sustained release property. Therefore, those clinical cases that demand biocompatibility, high dose coupled with a more stable release will benefit from it.

ACKNOWLEDGMENTS

This work was supported by the National Natural Science Foundation of China (51003025) and National High-Tech Research and Development Program (863 Program) (2013AA032302), as well as Hubei Provincial Natural Science Foundation (2014CFB547).

REFERENCES

1. Fu, C. H.; Liu, T. L.; Tang, F. Q.; Chen, D.; Li, L. L.; Liu, H. Y.; Li, X. M. *Chin. Sci. Bull.* **2012**, *57*, 2525.
2. Wu, X. L.; Tan, L. F.; Chen, D.; Meng, X. W.; Tang, F. Q. *Chem. Commun.* **2014**, *50*, 539.
3. Liu, H. Y.; Liu, T. L.; Wang, H.; Li, L. L.; Tan, L. F.; Fu, C. H.; Nie, G. J.; Chen, D.; Tang, F. Q. *Biomaterials* **2013**, *34*, 6967.
4. Fu, C. H.; Liu, T. L.; Li, L. L. *Biomaterials* **2013**, *34*, 2565.
5. An, F. Q.; Gao, B. J.; Dai, X.; Wang, M.; Wang, X. *J. Hazard. Mater.* **2011**, *192*, 956.
6. Zhang, K.; Xu, L. L.; Jiang, J. G.; Calin, N.; Lam, K. F.; Zhang, S. J.; Wu, H. H.; Wu, G. D.; Albela, B.; Bonneviot, L.; Wu, P. *J. Am. Chem. Soc.* **2013**, *135*, 2427.
7. Ji, J.; Shu, S.; Wang, F.; Liu, J.; Yu, Z. Z. *Colloids Surf. A* **2014**. *446*, 156.

8. Wu, Y.; Hu, D.; Su, Y. H.; Hsiao, Y. L.; You, B.; Wu, L. M. *Prog. Org. Coat.* **2014**, *77*, 1015.
9. Iacono, M.; Heise, A. *Polymers* **2015**, *7*, 1427.
10. Chen, J. C.; Liu, M. Z.; Chen, C.; Gong, H. H.; Gao, C. M. *Appl. Mater. Interfaces* **2011**, *3*, 3215.
11. Mandal, M.; Kruk, M. *Chem. Mater.* **2012**, *24*, 123.
12. Whitaker, K. A.; Furst, E. M. *Langmuir* **2014**, *30*,584.
13. Graf, C.; Vossen, D. L.; Imhof, A.; Blaaderen, A. V. *Langmuir* **2003**, *19*, 6693.
14. Wang, J. J.; Xiao, W.; Wang, J. Q.; Lu, J. M.; Yang, J. H. *Mater. Lett.* **2015**, *142*, 269.
15. Han, L.; Gao, C. B.; Wu, X. W.; Chen, Q. R.; Shu, P.; Ding, Z. G.; Che, S. N. *Solid State Sci.* **2011**, *13*, 721.
16. Richard, L. B.; Daniel, E. M. *Chem. Rev.* **2008**, *108*, 4915.
17. Yuan, J. J.; Mykhaylyk, O. O.; Ryan, A. J.; Armes, S. P. *J. Am. Chem. Soc.* **2007**, *129*, 1717.
18. Yang, J.; Lind, J. U.; Trogler, W. C. *Chem. Mater.* **2008**, *20*, 2875.
19. Zhou, F.; Li, S. H.; Vo, C. D.; Yuan, J. J.; Chai, S. G.; Gao, Q.; Armes, S. P.; Liu, C. J.; Cheng, S. Y. *Langmuir* **2007**, *23*, 9737.
20. Pi, M. W.; Yang, T. T.; Yuan, J. J.; Fujii, S.; Kakigi, Y.; Nakamura, Y.; Cheng, S. Y. *Colloids Surf. B* **2010**, *78*, 193.
21. Liu, P. X.; Chen, M.; Chen, C.; Fang, X. L.; Chen, X. L.; Zheng, N. F. *J. Mater. Chem. B* **2013**, *1*, 2837.
22. Patwardhan, S. V.; Clarson, S. J.; Perry, C. C. *Chem. Commun.* **2005**, *9*, 1113.
23. Brutchey, R. L.; Morse, D. E. *Chem. Rev.* **2008**, *108*, 4915.
24. Yuan, J. J.; Zhu, P. X.; Fukazawa, N.; Jin, R. H. *Adv. Funct. Mater.* **2006**, *2006*, 2205.
25. Patwardhan, S. V.; Clarson, S. *J. Mat. Sci. Eng. C* **2003**, *23*, 495.
26. Minati, L.; Antonini, V.; Serra, M. D.; Speranza, G.; Enrichi, F.; Riello, P. *Micropor. Mesopor. Mater.* **2013**, *180*, 86.
27. Kato, N.; Kato, N. *Micropor. Mesopor. Mater.* **2016**, *219*, 230.